Dyes and Pigments 82 (2009) 13–19

Contents lists available at ScienceDirect

Dyes and Pigments

journal homepage: www.elsevier.com/locate/dyepig

The synthesis, characterization, electrochemical character, catalytic and antimicrobial activity of novel, azo-containing Schiff bases and their metal complexes

Esin İspir

Department of Chemistry, Faculty of Science and Arts, Kahramanmaraş Sütçü İmam University, Kahramanmaraş 46050-9, Turkey

ARTICLE INFO

Article history:
Received 27 May 2008
Received in revised form
24 September 2008
Accepted 27 September 2008
Available online 14 October 2008

Keywords:
Schiff base complexes
Synthesis
Characterization
Catalysis
Redox studies
Antimicrobial activity

ABSTRACT

Three novel Schiff base ligands containing the azo group, 2-((*E*)-(4-((*E*)-phenyldiazenyl)phenylimino)methyl)phenol, 3-((*E*)-(4-((*E*)-phenyldiazenyl)phenylimino)methyl)benzene-1,2-diol and 4-((*E*)-(4-((*E*)-phenyldiazenyl)phenylimino)methyl)benzene-1,2,3-triol, were synthesized from the reaction of *p*-aminoazobenzene with salicylaldehyde, 2,4-dihydroxybenzaldehyde and 2,3,4-trihydroxybenzaldehyde, respectively. The mononuclear Co(II) and Cu(II) complexes of the Schiff base ligands were prepared and characterized using elemental analyses, IR, UV–visible spectroscopy, magnetic susceptibility and conductance measurements; ^{1}H NMR and mass spectra of the ligands were also recorded. The Co(II) and Cu(II) metal complexes are formed by the coordination of the N and O atoms of the ligands. The electrochemical properties of the metal complexes were investigated at 100 mV s^{-1} scan rate in DMSO; the oxidative C–C coupling properties of the Co(II) and Cu(II) complexes were investigated on the sterically hindered 2,6-di-*tert*-butylphenol (DTBP). In addition, the Schiff base ligands and their complexes were evaluated for both their in vitro antibacterial activity using the disc diffusion method.

1. Introduction

Azo compounds are versatile molecules and have received much attention in research both fundamental and application [1]. Apart from their purely chemical interest, azo-azomethine dyes are being increasingly used in the textile, leather, and plastic industries. Regarding the industrial importance of metallized azo dyes relative to their structures, they can be classified into two main types: those in which the azo group participates in coordination to the metal ion with formation of the chelate ring and those in which it is not [2].

Schiff bases derived from the salicylaldehydes are known as polydentate ligands, coordinating in deprotonated or neutral forms [1]. Schiff base ligands have significant importance in chemistry; especially in the development of Schiff base complexes, because Schiff base ligands are potentially capable of forming stable complexes with metal ions [3]. Many Schiff base complexes show excellent catalytic activity in various reactions at high temperature (>100 °C) and in the presence of moisture. Over the past few years, there have been many reports on their applications in homogeneous and heterogeneous catalysis, hence the need for a review article highlighting the catalytic activity of Schiff base complexes realized [4,5].

A wide variety of cobalt(II) complexes are known to bind dioxygen more or less reversibly and are therefore frequently studied as model compounds for natural oxygen carriers and for their use in O_2 storage, as well as in organic synthesis due to their catalytic properties under mild conditions. In this respect, Co(II) complexes with N-donor ligands containing binding units suitable either for the coordination of a single metal ion or for assembling dimetallic centers have been shown to be particularly useful [6]. In aprotic solvents, at atmospheric pressure and room temperature, cobalt chelated with Schiff bases catalyzes the oxygenation of indols, phenols, flavones, nitroalkanes, hydrazones, olefins, etc. [7].

In the first systematic study on the catalytic activity of model copper complexes towards the oxidation of 3,5-di-*tert*-butylcatechol (DTBC) which contemplated both mononuclear complexes and dinuclear complexes; Nishida et al. found that in some cases mononuclear complexes could be better catalysts than dinuclear ones, and stated that electrochemical data did not correlate in a direct manner to catalytic activity; the main conclusion in their paper was that distorted tetrahedral complexes were far more active than square-planar ones [8]. Later, comparing the reactivity of several mononuclear complexes with tripodal ligands, Malachowski concluded that both a convenient redox potential and a good steric match between substrate and catalyst are necessary for catalytic activity to be observed [9]. In addition, metal chelates play an essential role in the chemistry of living organisms and

---

E-mail address: esinispir@ksu.edu.tr

0143-7208/$ – see front matter © 2008 Elsevier Ltd. All rights reserved.
doi:10.1016/j.dyepig.2008.09.019

a large number of metal proteins and other metal complexes of biological importance have been studied [10].

Because of the importance of azo-containing Schiff base compounds and in continuance of the interest in syntheses of azo-based compounds, herein syntheses and characterization of a series of azo-linked salicylidenic Schiff bases named 2-((*E*)-(4-((*E*)-phenyldiazenyl)phenylimino)methyl)phenol (Hbab), 4-((1E)-(4-(phenyldiazenyl)phenylimino)methyl)benzene-1,3-diol (Dhbab) and 4-((*E*)-(4-((*E*)-phenyldiazenyl)phenylimino)methyl)benzene-1,2,3-triol (Thbab) and their metal complexes, are reported. The ligands in this study were synthesized by the reaction of *p*-aminoazobenzene with salicylaldehyde, 2,4-dihydroxybenzaldehyde and 2,3,4-trihydroxybenzaldehyde, respectively.

The Co(II) and Cu(II) complexes of these Schiff base ligands were also prepared and their structures were confirmed elemental analysis, IR and UV–visible spectral data. The analytical data shows that the metal to ligand ratio in the mononuclear Schiff base complexes is 1:2.

2. Experimental

2.1. Materials and measurements

All solvents were of reagent grade and were purified according to standard procedures. The metal salts [$Co(OAc)_2 \cdot 4H_2O$, $Cu(OAc)_2 \cdot H_2O$], salicylaldehyde, 2,4-dihydroxybenzaldehyde and 2,3,4-trihydroxybenzaldehyde were obtained from Fluka.

Elemental analyses were carried out by the Instrumental Analysis Laboratory of İnönü University. IR spectra were obtained using KBr discs (4000–400 cm^{-1}) on a Shimadzu 8300 FTIR spectrophotometer. The electronic spectra in the 200–900 nm range were obtained using THF on a Shimadzu UV-160 A spectrophotometer. Magnetic measurements were carried out by the Gouy method using $Hg[Co(SCN)_4]$ as calibrant. Molar conductances of the Schiff base ligands and their transition metal complexes were determined in MeOH ($\sim 10^{-3}$ M) at room temperature using a Jenway Model 4070 conductivity meter. Mass spectra of the ligands were recorded on a VG Zab Spec. GC–MS spectrometer with fast atom bombardment. ^{1}H NMR spectra were recorded on a Varian XL-200 NMR instrument. TMS was used as internal standard and deuteriated DMSO as solvent.

Cyclic voltammograms were recorded on a Iviumstat Electrochemical workstation equipped with a low current module (BAS PA-1) recorder. The electrochemical cell was equipped with a BAS glassy carbon working electrode (area 4.6 mm^2), a platinum coil auxiliary electrode and a Ag/AgCl reference electrode filled with tetrabutylammonium tetrafluoroborate ($[CH_3(CH_2)_3]_4NBF_4$, 0.1 M in DMSO, Aldrich) solution and adjusted to 0.00 V vs SCE. Cyclic voltammetric measurements were made at room temperature in an undivided cell (BAS model C-3 cell stand) with a platinum counter electrode and an Ag/AgCl reference electrode (BAS). The solutions were deoxygenated by passing dry nitrogen through the solution for 30 min prior to the experiments, and during the experiments the flow was maintained over the solution. Digital simulations were performed using DigiSim 3.0 for windows (BAS, Inc.). Experimental cyclic voltammograms used for the fitting process had the background subtracted and were corrected electronically for ohmic drop.

Catalysis experiments were monitored on a Shimadzu 160-A UV–visible spectrophotometer with a data station. Experiments were carried out using MeOH as solvent. In a generalized procedure a MeOH solution of 2,6-di-*t*-butylphenol (0.05 cm^3) and the complexes in a 50 cm^3 standard flask were kept under N_2. The compound 2,6-di-*t*-butylphenol (DTBP) was oxidized by aerial oxygen quantitatively to the 3,3′-5,5′-tetra-*t*-butyl-4,4′-diphenoquinone (TTBD) using the mononuclear complex as a catalyst. The change in the concentration of product 3,3′-5,5′-tetra-*t*-butyl-4,4′-diphenoquinone was monitored by optical spectroscopy.

2.2. Synthesis of 2-((E)-(4-((E)-phenyldiazenyl)phenylimino)methyl)phenol (Hbab)

The ligand 2-((*E*)-(4-((*E*)-phenyldiazenyl)phenylimino)methyl) phenol (Hbab), was prepared and characterized as described earlier [2]. UV–visible (in THF) (λ_{max}, nm, ε_{max}, M^{-1} cm^{-1}): 462 (2100), 367 (35,000), 348 (32,000). ^{1}H NMR (DMSO-d_6 δ ppm): 10.70 (s, 1 H, O-H), 8.91 (s, 1H, CH=N), 8.01 (d, *J* 3.10, 8.03 Hz, H-2, H-6), 7.65 (t, *J* 1.98, 8.21 Hz, H-3, H-4, H-5), 7.63 (d, *J* 2.54, 8.87, H-8, H-12), 7.61 (d, *J* 8.71, H-16), 7.52 (t, *J* 2.36, 8.81, H-17), 7.45 (t, *J* 2.36, 8.82, H-18), 7.02(d, *J* 8.86, H-19), 6.88 (d, *J* 2.34, 8.63, H-9, H-11). MS *m*/*z*: 302 (M + 1), 301 (M).

2.3. Synthesis of 4-((1E)-(4-(phenyldiazenyl)phenylimino)methyl)benzene-1,3-diol (Dhbab)

p-Aminoazobenzene (1.97 g, 10 mmol) dissolved in EtOH (10 cm^3) was carefully added with stirring to a solution of 2,4-dihydroxybenzaldehyde (1.38 g, 10 mmol) in EtOH (10 cm^3). The resulting mixture was allowed to stir magnetically under reflux for 2–3 h. After cooling the resulting precipitate was filtered, washed with cold EtOH, recrystallized from EtOH and dried in a vacuum dessicator. UV–visible (in THF) (λ_{max}, nm, ε_{max}, M^{-1} cm^{-1}): 463 (1808), 369 (29404), 348 (25,865). ^{1}H NMR (DMSO-d_6 δ ppm): 11.71 (s, 1 H, O-H), 10.63 (s, 1 H, O-H), 8.71 (s, 1H, CH=N), 8.18 (s, *J* 3.10, H-16), 8.01 (d, *J* 7.98, H-2, H-6), 7.65 (t, 1.98, 8.31, H-3, H-4, H-5), 7.53 (d, *J* 3.10, 8.80, H-9, H-11), 7.21 (d, *J* 2.71, 8.84, H-8, H-12), 6.95 (d, *J* 3.01, 8.81, H-18), 6.83 (d, *J* 8.80, H-19). MS *m*/*z*: 318 (M + 1), 317 (M).

2.4. Synthesis of 4-((E)-(4-((E)-phenyldiazenyl)phenylimino)methyl)benzene-1,2,3-triol (Thbab)

p-Aminoazobenzene (10 mmol, 1.97 g) and 10 mmol (1.54 g) of 2,3,4-trihydroxybenzaldehyde were condensed by refluxing in 70 cm^3 of absolute EtOH for 1 h. The solution was left at room temperature. The product was obtained as claret red microcrystals; the microcrystals were filtered off, washed with 10 cm^3 of absolute ethanol. UV–visible (in THF) (λ_{max}, nm, ε_{max}, M^{-1} cm^{-1}): 470 (1925), 361 (26,752), 343 (23,601). ^{1}H NMR (DMSO-d_6 δ ppm): 13.31 (s, 1H, O-H), 9.81 (s, 1H, O-H), 9.01 (s, 1H, O-H), 8.92 (s, 1 H, CH=N), 8.01 (d, *J* 3.10, 8.80, H-8, H-12), 7.93 (d, *J* 3.01, 8.80, H-9, H-11), 7.90 (d, *J* 7.82, H-2, H-6), 7.63 (t, *J* 1.93, 8.20, H-3, H-4, H-5), 7.20 (d, *J* 8.83, H-19), 6.46 (d, *J* 8.82, H-18). MS *m*/*z*: 334 (M + 1), 333 (M).

2.5. Synthesis of metal complexes

Hbab, Dhbab or Thbab ligand (20 mmol) dissolved in 40 cm^3 absolute EtOH was mixed with 10 mmol $Cu(Ac)_2 \cdot H_2O$ or $Co(Ac)_2 \cdot 4H_2O$ in 20 cm^3 EtOH. The stirred mixture was refluxed for 24 h, then evaporated to 15–20 cm^3 in vacuum and left to cool to room temperature. The compounds were precipitated after adding 5 cm^3 EtOH. The products were filtered in vacuum, washed with a small amount of MeOH and water, and recrystallized from EtOH. The products are soluble in solvents such as $CHCl_3$, DMF and DMSO.

2.6. Catalytic oxidation of 2,6-di-t-butylphenol

In a CH_2Cl_2/MeOH solvent mixture (1:1, 50 cm^3), the complexes [$Co(Hbab)_2$], [$Cu(Hbab)_2$], [$Co(Dhbab)_2$], [$Cu(Dhbab)_2$], [$Co(Thbab)_2$] and [$Cu(Thbab)_2$] were dissolved. To this solution, 2,6-di-*t*-butylphenol was added and the solution was stirred for 48 h; the ensuing mixture was filtered and the filtrate evaporated to dryness. MeOH (5 cm^3) were added to dissolve the excess 2,6-di-*t*-butylphenol. For measuring the progress of the reaction, 50 cm^3 from the aliquot was passed through an Amberlyst cationic ion-exchanger and washed with 10 cm^3 (2 × 5) CH_2Cl_2. The change in the

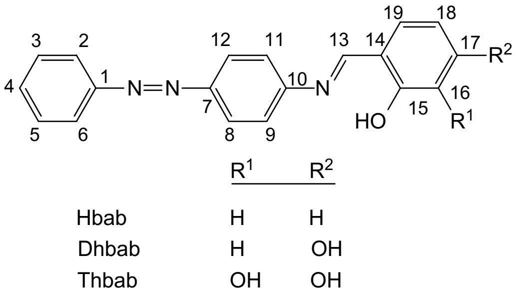

Fig. 1. The proposed structure of Schiff base ligands.

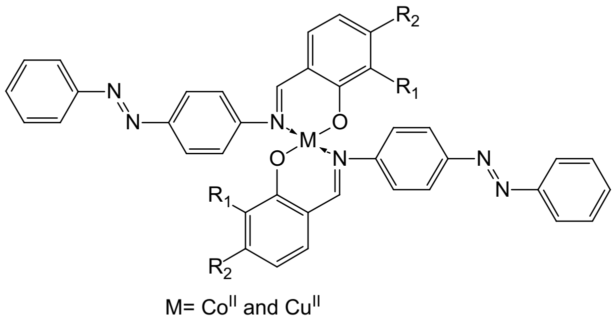

Fig. 2. The proposed structures of the Co(II) and Cu(II) complexes of ligands.

concentration of product 3,3′-5,5′-tetra-*t*-butyl-4,4′-diphenoquinone, was monitored by optical spectroscopy.

2.7. Redox studies

Cyclic voltammograms were recorded on an Iviumstat Electrochemical workstation equipped with a low current module (BAS PA-1) recorder. The electrochemical cell was equipped with a BAS glassy carbon working electrode (area 4.6 mm^2), a platinum coil auxiliary electrode and a Ag/AgCl reference electrode filled with tetrabutylammonium tetrafluoroborate ($[CH_3(CH_2)_3]_4NBF_4$, 0.1 M in DMSO, DMF and CH_3CN, Aldrich) solution and adjusted to 0.00 V vs SCE. Cyclic voltammetric measurements were made at room temperature in an undivided cell (BAS model C-3 cell stand) with a platinum counter electrode and an Ag/AgCl reference electrode (BAS). All potentials are reported with respect to Ag/AgCl. The solutions were deoxygenated by passing dry nitrogen through the solution for 30 min prior to the experiments, and during the experiments the flow was maintained over the solution. Digital simulations were performed using DigiSim 3.0 for windows (BAS, Inc.). Experimental cyclic voltammograms used for the fitting process had the background subtracted and were corrected electronically for ohmic drop.

2.8. Biological studies

The in vitro growth inhibitory activity of the ligands and their complexes were assigned against *Klebsiella pneumoniae* FMC 5, *Enterococcus cloacae* ATCC 13047, *Escherichia coli* ATCC 8739, *Bacillus megaterium* DSM 32, *Staphylococcus aureus* Cowan 1, *Micrococcus luteus* LA 2971, *Mycobacterium smegmatis* CCM 2067, *Pseudomonas aeruginosa* ATCC 27853, and their in vitro antifungal activity against *Candida albicans* ATCC 1023, *Kluyveromyces fragilis* A 230, *Rhodotorula rubra* by the disc diffusion method. All the bacteria mentioned above were incubated in Nutrient Broth (NB) (Difco) at 37 ± 0.1 °C for 24 h, and the yeasts were incubated in Sabouraud Dextrose Broth (SDB) (Difco) at 25 ± 0.1 °C for 48 h. The bacteria and yeasts (prepared as above) were injected into Petri dishes (9 cm) in the amount of 0.01 cm^3 (10^5/cm^3 for the bacteria and 10^3/cm^3 for the fungi), 15 ml of Mueller Hinton Agar (MHA, Oxoid) and Sabouraud Dextrose Agar (SDA) (sterilized in a flask and cooled to 45–50 °C) were homogenously distributed onto the sterilized Petri dishes [11]. All the compounds were injected into empty sterilized antibiotic discs having a diameter of 6 mm (Schleicher & Shüll No: 2668, Germany) in the amount of 30 μL. The compounds to be tested were dissolved in acetone to a final concentration of 2000 ppm and soaked in filter paper. Discs injected with complexes were located on the solid agar medium by pressing slightly. After Petri dishes so obtained were placed at 4 °C for 2 h, plates inoculated with fungi were incubated at 25 ± 0.1 °C for 24 h. At the end of the period, inhibition zones formed on the food medium were evaluated is millimeters [11]. These studies were performed in triplicate. Gentamicins (Bioanalyse) and Nystatin (Oxoid) were used as standards.

3. Result and discussion

3.1. Synthesis of the compounds

The Schiff base ligands, Hbab, Dhbab and Thbab have been prepared by the condensation between *p*-aminoazobenzene with salicylaldehyde, 2,4-dihydroxybenzaldehyde and 2,3,4-trihydroxybenzaldehyde, respectively, (1:1 molar ratio) in EtOH as shown in Fig. 1. The level of the purity of the ligands and the complexes was checked by T.L.C. on silica gel-coated plates. Hbab, Dhbab and Thbab Schiff base ligands give the complexes with Co(II) and Cu(II) salts. The complexes were synthesized by the general equations shown below.

The ligands are stable at room temperature and soluble in common organic solvents such as DMSO, DMF, EtOH and MeOH. The complexes are also stable at room temperature. Based on the elemental analyses, spectroscopic characterization, these mono-nuclear complexes are presumed to have the coordination

Table 1
Some analytical data and physical properties of ligands and their metal complexes.

Compound	Empirical formulas	Formula wt.	Colour	M.p. (°C)	Yield (%)	Calculated (Found) %			Λ[a]
						C	H	N	
Hbab	$C_{19}H_{15}N_3O$	301	Orange	160	84	75.73 (75.25)	5.02 (4.98)	13.94 (13.84)	1.1
$[Co(Hbab)_2]$	$C_{38}H_{28}CoN_6O_2$	658.9	Brown	260	84	69.20 (68.92)	4.25 (4.00)	12.75 (12.23)	10.1
$[Cu(Hbab)_2]$	$C_{38}H_{28}CuN_6O_2$	663.5	Dark Brown	245	78	68.73 (68.41)	4.22 (4.03)	12.66 (12.16)	11.2
Dhbab	$C_{19}H_{15}N_3O_2$	317	Pale orange	178	81	71.03 (71.91)	4.09 (4.76)	13.10 (13.24)	1.4
$[Co(Dhbab)_2]$	$C_{38}H_{28}CoN_6O_4$	691.6	Brownish red	225	79	65.99 (65.92)	4.08 (4.16)	12.15 (12.29)	11.3
$[Cu(Dhbab)_2]$	$C_{38}H_{28}CuN_6O_4$	696.2	Dark Orange	282	73	65.56 (66.11)	4.05 (4.01)	12.07 (12.12)	12.6
Thbab	$C_{19}H_{15}N_3O_3$	333.34	Claret red	215	78	68.46 (68.31)	4.54 (4.62)	12.61 (12.68)	1.3
$[Co(Thbab)_2]$	$C_{38}H_{28}CoN_6O_6$	723.60	Brown	235	71	69.07 (68.84)	3.90 (4.01)	11.61 (11.23)	12.1
$[Cu(Thbab)_2]$	$C_{38}H_{28}CuN_6O_6$	728.21	Dark Brown	271	75	62.68 (61.91)	3.88 (3.95)	11.54 (11.43)	13.2

[a] $\Omega^{-1}\,cm^3\,mol^{-1}$.

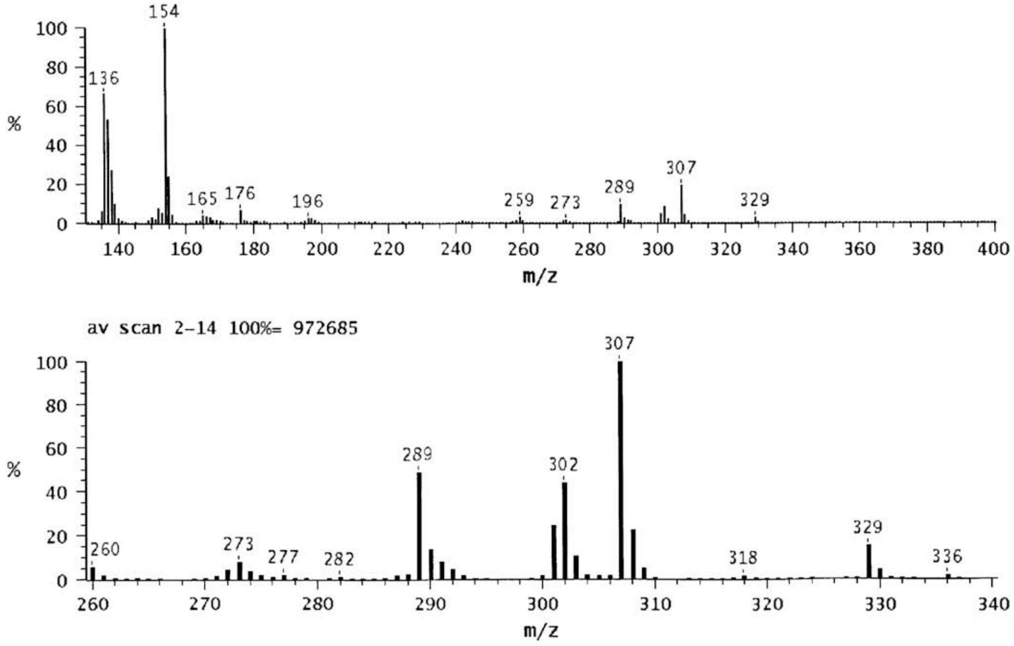

Fig. 3. The mass spectra of 2-((*E*)-(4-((*E*)-phenyldiazenyl)phenylimino)methyl)phenol (Hbab).

environment shown in Fig. 2. The structures of the complexes were elucidated with use of IR, UV–visible spectra and elemental analyses. Analytical data of ligands and their complexes are presented in Table 1. The experimental elemental analyses results of the complexes are in good compliance with the theoretical calculations. The data show the complexation of 1:2 [metal:ligand] ratio of the formulae of [M(L)$_2$]. Conductivity values for the [Co(Hbab)$_2$], [Cu(Hbab)$_2$], [Co(Dhbab)$_2$], [Cu(Dhbab)$_2$], [Co(Thbab)$_2$] and [Cu(Thbab)$_2$] compounds in MeOH are in the range of 10.15–13.21 (Ω^{-1} cm^3 mol^{-1}) indicating that they are non-electrolytes [12]. Single crystals of the compounds could not be isolated from any organic solution, thus no definite structures can be described. However, the analytical and spectroscopic data enables us to predict possible structures as shown in Fig. 1 and 2.

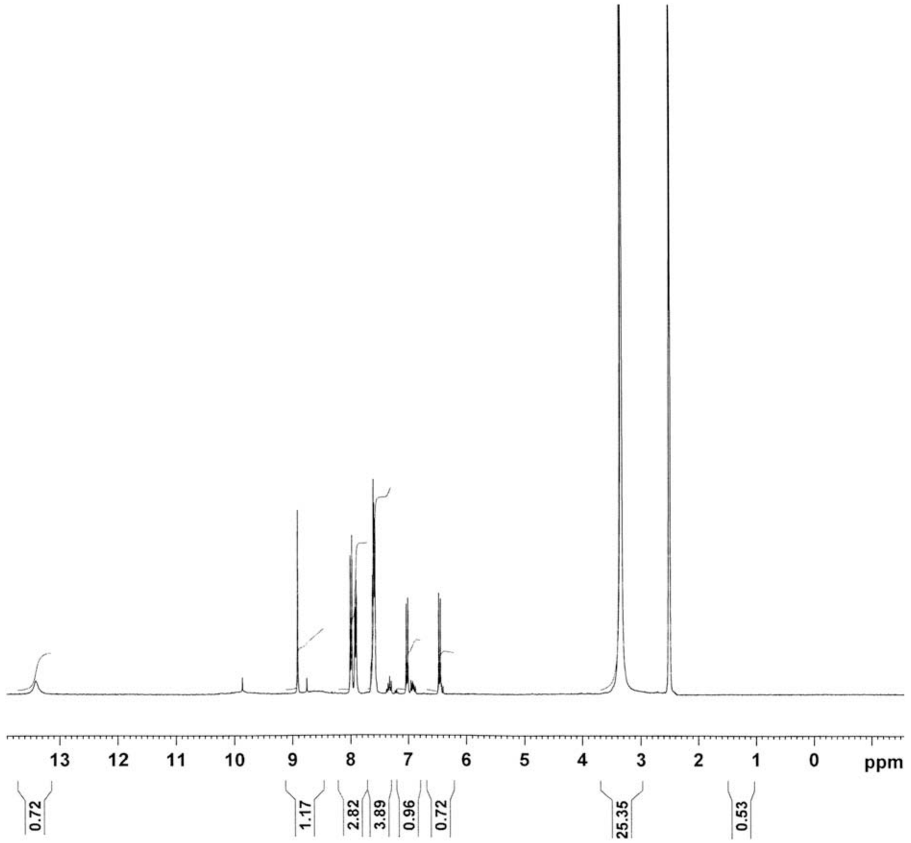

Fig. 4. The ^{1}H NMR spectrum of Thbab.

Table 2
Characteristic IR bands of the Schiff base ligands and their metal complexes (cm^{-1}, KBr).

Compound	ν(OH)	ν(ArC–H)	ν(CH=N)	ν(N=N)	ν(M–N)	ν(M–O)
Hbab	3425m	3055m	1614s	1591s	–	–
[Co(Hbab)$_2$]	–	3058m	1604s	1573s	422w	596m
[Cu(Hbab)$_2$]	–	3037m	1608s	1587m	418w	599m
Dhbab	3420	3057	1616	1598	–	–
[Co(Dhbab)$_2$]	3425	3056	1610	1581	419	589
[Cu(Dhbab)$_2$]	3427	3059	1612	1572	420	591
Thbab	3432	3056	1618	1595	–	599
[Co(Thbab)$_2$]	3428	3058	1609	1573	425	601
[Cu(Thbab)$_2$]	3431	3050	1613	1580	423	593

Table 3
UV–visible and magnetic moment data of the complexes in THF.

Compound	λ_{max}, nm (ε, M^{-1} cm^{-1})	μ_{eff}, BM
[Co(Hbab)$_2$]	630 (4647), 448 (9294), 361 (97,764), 274 (6411)	4.99
[Cu(Hbab)$_2$]	603 (1360), 490 (1560), 361 (30,680), 265 (10,350)	1.65
[Co(Dhbab)$_2$]	643(138), 422 (9325), 355 (76,605), 246 (91,771)	5.13
[Cu(Dhbab)$_2$]	620 (40), 463(23,740), 361 (35,900), 267 (5660)	1.74
[Co(Thbab)$_2$]	662 (185), 490 (1259), 365 (57,741), 283 (12,519)	5.28
[Cu(Thbab)$_2$]	617 (4), 465 (7142), 370 (6558), 275 (352)	1.78

3.2. *Mass spectrum of the ligands*

In the mass spectrum of the ligands, the peaks observed at m/z 301, 317 and 333 can be assigned to the molecular ions M^+ and the peaks at *m*/*z* 302, 318 and 334 to the $[M+1]^{+1}$ ions [2]. The most intense peaks at *m*/*z* 289, 305 and 321 corresponds to $[C_6H_4–N{=}N–C_6H_4–N{=}CH–C_5H_4OH]^+$, $[C_6H_4–N{=}N–C_6H_4–N{=}CH–C_5H_4(OH)_2]^+$, and $[C_6H_4–N{=}N–C_6H_4–N{=}CH–C_5H_4(OH)_3]^+$, which results from loss of one carbon atoms from the parent ligands. The other important peaks at *m*/*z* 273–154 and *m*/*z* 289–170 may be assigned to the loss of the oxygen and the $[C_6H_4–N{=}N]^+$ fragments. The mass spectrum of Hbab ligand is taken as a representative example and shown in Fig. 3.

3.3. *^{1}H NMR spectrum of the ligands*

The ^{1}H NMR spectra of the Thbab ligand is taken as a representative example and shown in Fig. 4.

In the ^{1}H NMR spectra of the Hbab, Dhbab and Thbab ligands, the singlets in the 10.70–9.01 ppm range can be attributed to the proton of the first –OH group which is neighboring in the azomethine group. In addition, the second –OH group of Dhbab and Thbab moiety is shown at 11.71 and 13.31 ppm as a singlet, respectively. The third –OH group of THbab is shown at 9.81 ppm as a singlet too. The OH peaks disappear together with addition of the D_2O [12]. All three ligands exhibit singlet signals in the 8.8–8.9 ppm range which are attributed to the azomethine group protons, respectively [13]. The ^{1}H NMR spectra of ligands in DMSO-d_6 revealed a multiplet at 6.5–8.0 ppm corresponding to aromatic protons [4].

3.4. *IR spectra*

The characteristic IR data of the Schiff base ligands and their metal complexes listed in Table 2.

In order to study the binding of Schiff base ligands to the metal in the complexes, the IR spectrum of the free Schiff base ligands were compared with that of the metal complexes. In the ligands and complexes spectra, both ligands and complexes exhibit bands at 3409–3425 cm^{-1} and 3075–3038 cm^{-1} that are assignable to ν(OH) and ν(Ar–CH) [14, 15]. In the complexes, two of the four coordination sited of metal ions were occupied by two nitrogen atoms of the azomethine groups; the other two groups were hydroxyl ions. Because of this, in the complexes of the (Hbab) ligand, the ν(OH) vibration was disappeared. In the other complex spectrums, the ν(OH) vibrations attributed to the OH groups which were not coordinated with metal ions were unchanged. The bands at 1641–1643 cm^{-1} is due to the vibration of the azomethine group (–CH=N–) in both ligands. Metal complexes show significant differences from ligands [16,17]. After coordination between Schiff base ligands and Co(II)–Cu(II) metal salts, the C=N stretching frequencies slightly shift to lower wave number region. The lowering of frequencies of the C=N peak is indicative of the formation of metal–ligand bonds [18]. In the complexes, new weak bands in the 611–563 and 445–418 cm^{-1} range may be attributed to ν(M–O) and ν(M–N) stretching [19].

3.5. *UV–visible spectra*

The electronic absorption spectral data for complexes were obtained in 10^{-3} M THF solutions at room temperature and magnetic moment data are given in Table 3. The UV–visible spectra of the Schiff base ligands and their metal complexes in THF showed absorption bands between 662 and 246 nm. The spectra of the complexes show intense bands in the high-energy region at 306–370 nm which can be assigned to charge transfer L → M bands [20,21]. The bands at λ_{max} 470, 463 and 462 nm assigned to $n \rightarrow \pi^*$ transitions of the azomethine groups in the (Hbab), (Dhbab) and (Thbab) ligands. In the spectra of the complexes, the bands of the azomethine $n \rightarrow \pi^*$ transitions are shifted to lower frequencies indicating that the imine nitrogen atom is involved in coordination to the metal ion. The spectra of all complexes contain an absorption band in the 662–603 nm range may be assigned to the d–d transition of metal ions [22]. The Co(II) complexes show bands at 630, 643 and 662 nm. This indicates tetrahedral geometry for the Co(II) complexes. In general, due to Jahn–Teller distortion, square-planar Cu(II) complexes give a broad absorption band between 600 and 700 nm. In the electronic spectra of Cu(II) complexes, the observed bands are 603, 617 and 620 nm. [23]. These values suggest square-planar geometry for Cu(II) complex.

The magnetic moments (Table 3) of the copper(II) complexes all fall in the normal range for a copper(II) species with $S = 1/2$. Magnetic moment values vary from 1.65–1.78 B.M. and this confirms that the copper(II) complexes have square-planar geometry. The values of 4.99, 5.13 and 5.28 B.M. observed for [Co(Hbab)$_2$], [Co(Dhbab)$_2$] and [Co(Thbab)$_2$] reveal tetrahedral geometry around the Co(II) ion [2].

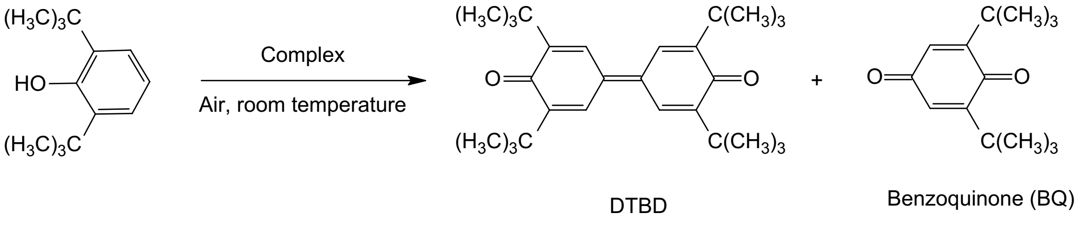

Fig. 5. Oxidative C–C coupling reaction of the sterically hindered phenol 2,6-di-*t*-butylphenol.

3.6. Catalytic activity

The catalytic activities of the mononuclear complexes [Co(Hbab)$_2$], [Cu(Hbab)$_2$], [Co(Dhbab)$_2$], [Cu(Dhbab)$_2$], [Co(Thbab)$_2$] and [Cu(Thbab)$_2$] were examined for oxidation of 2,6-di-*t*-butylphenol by air O_2 to 2,2′-di-*t*-butyl-4,4′-diphenolquinone (TTBD) in air saturated DCM according to the reaction in Fig. 5.

All complexes in the catalysis reaction are soluble in the DCM-methanol solvent mixture. If they are not also soluble in this mixture, there is no problem, because, this type reactions can occur at the heterogen or homogen phase in the similar way. As the oxidative carbon–carbon coupling of the sterically hindered phenol 2,6-di-*t*-butylphenol lead to diphenoquinones is in radical mediated reactions, the mononuclear Co(II) and Cu(II) complexes have been studied for oxidative studies with 2,6-di-*t*-butylphenol. When the phenols (2 mmol) are added to the complexes (0.01 mmol) in DCM-MeOH (1:1) solvent mixture (50 cm^3), the dark brown or black turns to red or light red in the presence of air. It was found that after 55–78 h, the phenol compound was converted to the 3,3′4-5,5′-tetra-*t*-butyl-4,4′-diphenolquinone for the complexes.

For the compound 2,6-di-*t*-butylphenol, the best oxidant is the complexes of the ligand Thbab and moreover, the complexes of the ligand Hbab are the worst oxidant for the sterically hindered phenol. These two different situations can be explained by the properties of the ligands. In the ligand Thbab, there are three –OH groups and these groups have more electron-donor properties with a mesomeric effect than other ligands and therefore the activity of the complexes increases. In other words, in the ligands Dhbab and Hbab, the number of the –OH groups are decrease. For this reason the activity of ligands Dhbab and Hbab decrease, respectively [12].

Order of the oxidizing of the complexes is: [Co(Hbab)$_2$] > [Cu(Hbab)$_2$] > [Co(Dhbab)$_2$] > [Cu(Dhbab)$_2$] > [Co(Thbab)$_2$] > [Cu(Thbab)$_2$]. The spectral properties of the complexes are shown in Fig. 6. The course of the reaction was followed by optical spectroscopy, as TTBD shows a characteristic peak in the electronic spectrum at 425 nm, as seen also from Fig. 6. Such changes in the electronic spectra of the complexes at different time intervals were monitored by removing the catalyst from the reaction solution. At the end of the oxidative coupling, the properties of the complexes changed.

3.7. Electrochemical studies

The redox properties of the Co(II) and Cu(II) complexes of (Hbab), (Dhbab) and (Thbab) were investigated by cyclic voltammetry (Table 4) in the potential range +2.0 to −2.0 V. DMSO solution was used as the solvent and tetrabutylammonium perchlorate as the supporting electrolyte at a scan rate of 100 mV s^{-1}. The cyclic voltammerty (CV) curve of the [Co(Hbab)$_2$] complex is given in Fig. 7.

Table 4
Electrochemical data for the obtained complexes.

Compound	E_{pa} (V)	E_{pc} (V)	ΔE (V)	$E_{1/2}$ (V)
[Co(Hbab)$_2$]	0.400, −0.140	−0.030	0.430	–
[Cu(Hbab)$_2$]	−0.540, 0.090, −0.580	0.120, 0.420, 0.830	−0.660, −0.330	–
[Co(Dhbab)$_2$]	−0.080, −0.520	0.870, −0.270	−0. 950	–
[Cu(Dhbab)$_2$]	−0.640, 0.030	1.080, −0.070	−1.720	–
[Co(Thbab)$_2$]	0.220, −0.490	−0.010, −0.550	0.230, 0.060	0.105
[Cu(Thbab)$_2$]	0.030, −0.930	−0.670, −0.120	0.700, −0.810	–

Supporting electrolyte: [NBu$_4$](ClO$_4$) (0.05 M); concentrations of the compounds: 0.001 M. All the potentials are referenced to Ag/AgCl; where *E*pa and *E*pc are anodic and cathodic potentials, respectively. $E_{1/2} = 0.5 \times (Epa + Epc)$, $\Delta Ep = Epa - Epc$. The data have been obtained at 100 mV s^{-1} scan rate.

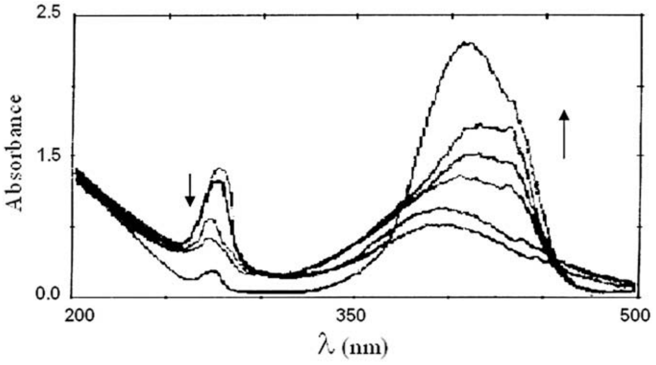

Fig. 6. Electronic spectra of the eluted solutions at different time intervals for the aerial oxidation of DTBP to TTBD using complexes as catalysts.

As seen from electrochemical curves and data, the [Co(Hbab)$_2$] complex shows two anodic an done cathodic peaks in the −0.03 to +0.40 V range. The [Co(Hbab)$_2$] complex has an irreversible character. In other words, the [Co(Thbab)$_2$] complex has $|Ip_a{:}Ip_c| \cong 0.9$ ratio. This value shows that the [Co(Thbab)$_2$] complex has a quasi-reversible character. The separation of the anodic and cathodic peak potentials, $Ep_c = 100$ mV, and the ratio of anodic to cathodic peak currents indicate a quasi-reversible redox potentials [24]. All other complexes have irreversible character and their oxidation reduction peaks' range is in the 1.080 to −0.930 V. In the irreversible electrochemical processes of the divalent metals:

$$M(II) + \xrightarrow{e^-} M(I) + \xrightarrow{e^-} M(O)$$

In the [Co(Hbab)$_2$] complex, this process is as given below:

$$Co(II) + e^- \underset{-e^-}{\leftrightarrows} Co(I) + e^- \underset{-e^-}{\leftrightarrows} Co(O)$$

3.8. Biological activity

The Hbab, Dhbab and Thbab ligands and their metal complexes were tested for their inhibitory effects on the growth of *K. pneumoniae*, *E. cloacae*, *E. coli*, *B. megaterium*, *S. aureus*, *M. luteus*, *M. smegmatis*, *P. aeruginosa* bacteria and *C. albicans*, *K. fragilis* and *R. rubra* fungi because bacteria can achieve resistance to antibiotics through biochemical and morphological modifications [25]. The antimicrobial activity was tested by using the disc diffusion

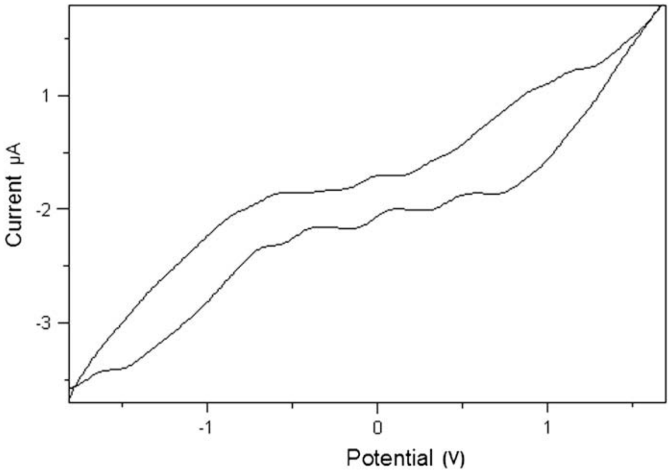

Fig. 7. Cyclic voltammograms of the complex [Co(Hbab)$_2$].

Table 5
Antimicrobial activity studies of ligands and their metal complexes [diameter of inhibition zone (mm); concentration 2000 ppm, 30 μL/disc].

Compound	Inhibition zone (mm)										
	Bacteria								Fungi		
	Klebsiella pneumoniae	*Enterococcus cloacae*	*Escherichia coli*	*Bacillus megaterium*	*Staphylococcus aureus*	*Micrococcus luteus*	*Mycobacterium smegmatis*	*Pseudomonas aeruginosa*	*Candida albicans*	*Kluyveromyces fragilis*	*Rhodotorula rubra*
Hbab	0	0	0	0	0	0	0	0	0	7	8
[Co(Hbab)$_2$]	0	0	0	0	0	0	0	0	0	14	15
[Cu(Hbab)$_2$]	0	0	0	0	0	0	0	0	0	10	9
Dhbab	0	0	0	0	0	0	0	0	0	8	10
[Co(Dhbab)$_2$]	0	0	0	0	0	0	0	0	0	8	10
[Cu(Dhbab)$_2$]	0	0	0	0	0	0	0	0	0	7	11
Thbab	8	8	7	7	9	9	8	8	0	0	0
[Co(Thbab)$_2$]	7	8	7	7	8	9	8	7	9	9	8
[Cu(Thbab)$_2$]	7	8	8	8	8	9	8	7	7	7	8

method. The antibacterial and antifungal activities of the new compounds are presented in Table 5.

The results indicate that the complexes show more activity and the ligands do not have any activity against same microorganisms under identical experimental conditions. This would suggest that the chelation could facilitate the ability of a complex to cross a cell membrane and can be explained by Tweedy's chelation theory [26]. Chelation considerably reduces the polarity of the metal ion because of partial sharing of its positive charge with donor groups and possible electron delocalization over the whole chelate ring. Such a chelation could enhance the lipophilic character of the central metal atom, which subsequently favors its permeation through the lipid layer of the cell membrane. The variation in the effectiveness of different compounds against different organisms depends either on the impermeability of the cells of the microbes or on differences in ribosome of microbial cells.

Hbab, Dhbab, [Co(Hbab)$_2$], [Cu(Hbab)$_2$], [Co(Dhbab)$_2$] and [Cu(Dhbab)$_2$] have no activity against bacteria and have activity against fungi. On the contrary, the Thbab ligand has activity against bacteria and has no activity against fungi. The remarkable activity of the Thbab ligand may arise from excess of the hydroxyl groups, which may play an important role in antibacterial activity [6]. [Co(Thbab)$_2$] and [Cu(Thbab)$_2$] complexes have activity against both bacteria and fungi. Of the complexes tested, [Co(Hbab)$_2$] exhibited higher activity against *K. fragilis* and *R. rubra* than the other complexes but has no antibacterial activity against all tested bacteria. The variation in the activity of the metal complexes against different organisms depends on the impermeability of the microorganism cells or on differences in ribosome of microbial cells [27].

4. Conclusions

Three novel Schiff base ligands containing –N=N– group, 2-((*E*)-(4-((*E*)-phenyldiazenyl)phenylimino)methyl)phenol (Hbab), 3-((*E*)-(4-((*E*)-phenyldiazenyl)phenylimino)methyl)benzene-1,2-diol (Dhbab) and 4-((*E*)-(4-((*E*)-phenyldiazenyl)phenylimino)methyl) benzene-1,2,3-triol (Thbab) (Fig. 1), were synthesized from the reaction of *p*-aminoazobenzene with salicylaldehyde, 2,4-dihydroxybenzaldehyde and 2,3,4-trihydroxybenzaldehyde and their mononuclear Co(II) and Cu(II) complexes have been prepared. According to the analytical, UV–visible and IR data, the Co(II) and Cu(II) metal complexes are formed by the coordination of *N*, *O* atoms of the ligands. The catalytic activity of the mononuclear complexes [Co(Hbab)$_2$], [Cu(Hbab)$_2$], [Co(Dhbab)$_2$], [Cu(Dhbab)$_2$], [Co(Thbab)$_2$] and [Cu(Thbab)$_2$] has been examined for oxidation of 2,6-di-*t*-butylphenol by air O_2 to 2,2′-di-*t*-butyl-4,4′-diphenolquinone (DTBD) in air saturated DCM according to the reaction in Fig. 7. Order of the oxidizing of the complexes is: [Co(Hbab)$_2$] > [Cu(Hbab)$_2$] > [Co(Dhbab)$_2$] > [Cu(Dhbab)$_2$] > [Co(Thbab)$_2$] > [Cu (Thbab)$_2$]. The redox studies showed that all complexes, except [Co(Thbab)$_2$] complex, have irreversible character. The [Co(Thbab)$_2$] complex has quasi-reversible character. In addition, the antimicrobial activity study indicates that the complexes show more activity and the ligands do not have any activity against same microorganisms under identical experimental conditions.

Acknowledgements

The author thanks Dr. Mehmet Tümer (K. Maraş Sütçü Imam University, Chemistry Department) for the electrochemical studies and Dr. Sevil Toroğlu (K. Maraş Sütçü Imam University, Biology Department) for the antimicrobial studies.

References

[1] Nejati K, Rezvani Z, Massoumi B. Dyes Pigments 2007;75:653.
[2] Peker E, Serin S. Synth React Inorg Met-Org Chem 2004;34:859.
[3] Souza P, Garcia-Vazquez JA, Masaguer JR. Transition Met Chem 1985;10:410.
[4] Naeimi H, Safari J, Heidarnezhad A. Dyes Pigments 2007;73:251.
[5] Lippard SJ, Berg JM. Principles of bioinorganic chemistry. California: University Science Books; 1994.
[6] Tümer M, Ekinci D, Tümer F, Bulut A. Spectrochim Acta Part A 2007;67:916.
[7] Pui A, Berdan I, Morgenstern-Badarau I, Gref A, Perrée-Fauvet M. Inorg Chim Acta 2001;320:167.
[8] L'Argentiere PC, Cagnola EA, Quitoga ME, Liprandi DA. Appl Catal A 2002;226:253.
[9] Ispir E, Kurtoğlu M, Toroğlu S. Synth React Inorg Met-Org Chem 2004;36:627.
[10] Kurtoğlu M, İspir E, Kurtoğlu M, Serin S. Dyes Pigments 2008;77:75.
[11] Collins CH, Lyne PM, Grange JM. Microbiological methods. London: Butterworths; 1989. 410.
[12] Tümer Mehmet, Deligönül Nihal, Gölcü Aysegül, Akgün Eyüp, Dolaz Mustafa, Demirelli Havva, Diğrak Metin. Transition Met Chem 2006;31:12.
[13] Odabaşoğlu M, Arslan F, Ölmez H, Büyükgüngör O. Dyes Pigments 2007;75:507.
[14] Sanmartin J, Bermejo MR, Gariç-Deibe AM, Maneiro M, Large C, et al. Polyhedron 2000;19:185.
[15] Jaworska JK. Transition Met Chem 1994;19:296.
[16] Abbasi AR, Rezvani Z, Nejati K. Dyes Pigments 2006;70:71.
[17] Odabaşoğlu M, Albayrak Ç, Özkanca R, Akyan FZ, Lonecke PJ. Mol Struct 2007;840:71.
[18] Ispir E, Kurtoğlu M, Purtaş F, Serin S. Transition Met Chem 2005;30:1042.
[19] El-Saied FA, Ayad MI, Aly SA. Transition Met Chem 1999;18:279.
[20] Cazacu M, Marcu M, Vlad A, Vasiliu M. J Macromol Sci Part A Pure Appl Chem 2004;41:565.
[21] Kurtoğlu M, Ispir E, Kurtolu N, Toroğlu S, Serin S. Transition Met Chem 2005;30:765.
[22] Çakır S, Biçer E, Odabaşoğlu M, Albayrak Ç. J Braz Chem Soc 2005;4:711.
[23] Sallam SA. Transition Met Chem 2006;31:47.
[24] Tümer M. J Coord Chem 2007;60:2051.
[25] Mandal S, Nag K. J Chem Soc Dalton Trans 1983:2429.
[26] Tweedy BG. Phytopathalogy 1964;55:910.
[27] Sengupta SK, Pandey OP, Srivastava BK, Sharma VK. Transition Met Chem 1998;23:349.